Energy Technology
Generation, Conversion, Storage, Distribution
www.entechnol.de

Adjustment of Electrolyte Composition for All-Vanadium Flow Batteries and Its Effect on the Thermal Stability of Electrolyte for Positive and Negative Half-Cells

Nataliya V. Roznyatovskaya, Matthias Fühl, Martin Joos, Jens Noack, Peter Fischer, Karsten Pinkwart, and Jens Tübke*

Commercial electrolyte for vanadium flow batteries is modified by dilution with sulfuric and phosphoric acid so that series of electrolytes with total vanadium, total sulfate, and phosphate concentrations in the range from 1.4 to 1.7 M, 3.8 to 4.7 M, and 0.05 to 0.1 M, respectively, are prepared. The electrolyte samples of the series for positive and negative half-cells at various state-of-charges are produced by electrolysis and are investigated for stability in the range of temperatures from −20 to +65 °C. It is attempted to reveal a correlation between initial electrolyte formulation in terms of total vanadium and total sulfate concentrations, which are measurable parameters in practice, and electrolyte thermal stability properties. The study of negative electrolyte samples by headspace online mass spectrometry enables to detect hydrogen gas, which evolves by chemical reaction of vanadium(II) species with protons during thermally induced aging. The battery with vanadium electrolyte at 1.4 M total vanadium, 4.7 M total sulfate, and 0.1 M phosphate concentrations displays more stable operation in terms of capacity decay during galvanostatic charge–discharge cycles than the battery with electrolyte at 1.7 M vanadium, 3.8 M sulfate, and 0.05 M phosphate concentrations under the same conditions.

1. Introduction

Flow batteries (FBs) are currently applied for conversion and storage of renewable energy in large grids to reduce the consumption of fossil fuels for energy conversion and thereby to reduce the carbon dioxide emissions. Moreover, the FBs have been recently reported to be used in a double function, i.e., as power supply and heat management for microelectronic devices, where the electrolyte of FB serves simultaneously as a heat exchanger for the management of the thermal load of the electronics.[1]

All-vanadium FB (VFB) is one of the flow-battery technologies, which is the most investigated and is already commercialized. However, the double-function application of VFB is limited by low thermal stability of vanadium electrolyte, which, in turn, results from specific and complex chemistry of vanadium species. This limitation of electrolyte stability at temperatures typically over 35–40 °C is caused by irreversible precipitation of solid vanadium pentoxide in positive electrolyte at elevated temperatures and reversible precipitation of vanadium salts in negative electrolyte at low temperatures. During long-term operation of kW-scale VFBs at higher currents (40–400 A) in the absence of active cooling, the temperature of both positive and negative electrolyte in the tanks can increase from 35 up to 50 °C. The maximal temperature is attained at the end of the discharge and the decrease of the temperature occurs during the charge.[2] Thus, industrial-scale VFBs should be equipped by relevant thermal management or cooling system, which reduces the round-trip efficiency of the system and increases the investment cost.

The thermal management of heat generated inside the battery stack during VFB charge–discharge operation can be carried out also by electrolyte flow-rate optimization.[3] The enhancement of the thermal stability of vanadium electrolyte in a broad temperature operation range is achieved by adjustment of electrolyte composition, i.e., by the choice of the nature and amount of acid and additives.[4] The role of acid is considered in the literature mostly in the context of chemical stabilization of positive electrolyte at elevated temperatures, containing vanadium(V) and vanadium(IV) species. Quantitative guidelines on tailoring vanadium electrolyte specifications to specific use conditions have been given by Buckley et al.[5] The authors analyzed the effect of changing concentration of vanadium and sulfates to

N. V. Roznyatovskaya, M. Fühl, M. Joos, J. Noack, P. Fischer, K. Pinkwart, J. Tübke
Applied Electrochemistry
Fraunhofer Institute for Chemical Technology
Joseph-von-Fraunhofer-Str. 7, 76327 Pfinztal, Germany
E-mail: nataliya.roznyatovskaya@ict.fraunhofer.de

N. V. Roznyatovskaya, J. Noack, P. Fischer, K. Pinkwart, J. Tübke
German-Australian Alliance for Electrochemical Technologies for Storage of Renewable Energy (CENELEST)
Mechanical and Manufacturing Engineering
University of New South Wales (UNSW)
UNSW Sydney
Sydney, NSW 2052, Australia

DOI: 10.1002/ente.202300739

counteract the decrease in the stability of positive electrolyte at higher temperatures and derived expressions to calculate the necessary concentrations using the example of electrolyte without stabilizing additives such as phosphoric acid.

As electrode reactions of V(V)/V(IV) redox couple in positive half-cell are proton-dependent, i.e., protons are consumed or released during vanadium electrode reactions, a stable VFB operation requires ions transfer across the membrane to maintain proton mass balance between the positive and negative half-cells.[6] Liu et al.[7] have introduced the concept of vanadium to proton ratio (C_V/C_H) to investigate the effect of total vanadium concentration (C_V) in electrolyte on VFB performance. The amount of protons (C_H) or free acid in positive and negative half-cells depends generally on the way of electrolyte production, i.e., total amount of sulfate (C_S) (the total sulfate amount (C_S) is the sum of the concentrations of sulfate, bisulfate species, and free sulfuric acid, which are constituents of vanadium electrolyte solution. To avoid misunderstanding, C_S and free acid concentrations are not always equal to the amount of acid used to dissolve vanadium compounds for electrolyte preparation; however, there is a correlation between all these parameters) and on the type of membrane and side reactions.[8] Reducing C_V/C_H ratio can slow down the electrolyte imbalance, capacity decay, and side reactions in long-term VFB operation as it was demonstrated by the example of VFB operated with electrolyte of 1.5 and 1.8 M vanadium concentrations.[7]

Electrolyte composition in terms of C_V, C_S, or C_H has direct impact on the physicochemical properties of electrolyte such as conductivity, viscosity, density and in turn it has an effect on important performance indicators such as practical energy density, energy efficiency (EE), ohmic, kinetic, and transport losses.[7] Increase in vanadium concentration results in an approximately linear increase in density, viscosity, and volumetric capacity, but decrease in conductivity.[7] To reduce electrolyte resistance, which can account for 70% of the cell resistance, Song et al.[9] suggested to operate VFB with diluted electrolyte at C_V of 0.5 M at higher temperature of 50 °C. Electrolyte at C_V of 1.6 M and C_S of 4.4 M exhibited the best performance in terms of minimal discharge capacity decay at current densities of 50–100 mA cm^2 and highest EE compared to other electrolytes under consideration at C_V and C_S in the range from 1.4 to 2.2 M and 3.8 to 5 M correspondingly.[10]

In contrast to the positive electrolyte, the effect of vanadium electrolyte composition on the electrolyte stability in negative half-cell is less investigated. The lower potential of V(III)/V(II) redox couple thermodynamically allows for simultaneous hydrogen evolution reaction (HER) on the negative electrode of the VFB. The thermodynamic force of HER reaction increases with an increase in proton concentration (C_H) in vanadium electrolyte, and the rate of HER reaction is more largely influenced by operating temperature than V(III)/V(II) electrode reaction.[11,12] The opinions about the origin of HER reaction are controversial. Lee et al. assume that HER reaction is catalyzed by adsorbed V(II) species formed via hydrolysis.[13] Recently, Greese et al. demonstrated that adsorbed V(II) species inhibit HER.[14] In contrast to electrochemical HER, homogeneous reaction of V(II) with water to evolve hydrogen in negative electrolyte is commonly considered as decelerated or kinetically limited. Static thermal stability test based on visual inspection of positive and negative electrolyte samples exposed to a preset temperature for 7 days showed that the stability is limited by recrystallization of V(II) species at low temperatures (down to −35 °C) and precipitation of V(V) species at high temperatures (up to 60 °C).[15] Other authors report about precipitation of V(III) from negative electrolyte solution at low temperatures or after the long-term storage at room temperature and recommend electrolyte solutions in C_S in the range from 4 to 5 M[16] or 3 to 4 M[17] for C_V of 1.5–1.6 M.

In this study, we modify the composition of commercial vanadium electrolytes by changing the C_V, C_S as well as an amount of phosphoric acid as additive and investigate the effect of this modification on ex situ thermal stability of both of the positive and negative electrolytes. Special attention is given to examination of hydrogen evolution caused by homogeneous side reaction of V(II) species with water.

2. Results and Discussion

2.1. Preparation of Electrolyte Series

The modification of vanadium $V^{3.5+}$ electrolyte composition was carried out under the following considerations. First, the concentration of phosphate additive (C_P) in electrolytes containing about 1.6 M vanadium is often in the range from 0.05 to 0.1 M[18] to stabilize positive electrolyte at higher temperatures. Moreover, some electrolyte producers use phosphoric acid additive in commercial electrolyte or add it if required by consumer. Therefore, a part of modified electrolytes series contained about 0.05 M of phosphate and another part of electrolytes was prepared by adjustment of phosphate concentration at 0.1 M (**Figure 1**, **Table 1**).

The C_S value for vanadium electrolytes based on sulfuric acid is commonly in the range from 3 to 5 M according to the published data. The modification of electrolyte composition in this study includes consideration and variation of C_V/C_S ratio for the electrolyte composition by addition of acid and/or dilution of electrolyte. Such procedure results from a practical concern that it can be easier to modify a commercial electrolyte by dilution and addition of acids than to prepare the electrolyte with the preset C_V and C_S values from raw vanadium compounds. As shown in Figure 1, the conductivity of modified electrolyte samples

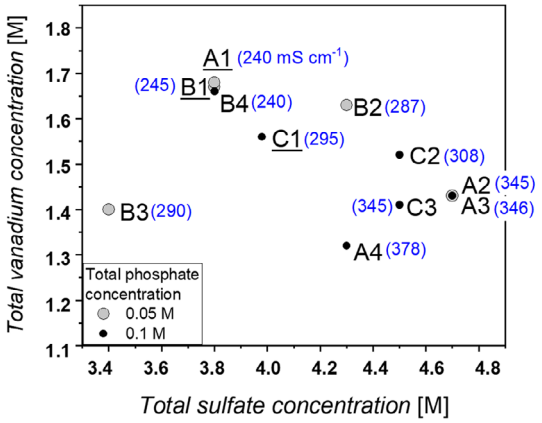

Figure 1. Abbreviations for series of $V^{3.5+}$ electrolyte samples used in the work indicate the total vanadium and sulfate concentration. The commercial electrolyte samples in $V^{3.5+}$ form are underlined. Conductivity data are shown in brackets and given in mS cm^{-1}.

Table 1. Composition of vanadium electrolyte samples used in the study. The commercial electrolyte batches are underlined.

Sample of $V^{3.5+}$ electrolyte	Molar content [%]		Total concentration [M]			Conductivity [mS cm^{-1}]	Comment
	V(III)	V(IV)	Vanadium	Sulfate	Phosphate		
A1	48.3	51.7	1.68	3.8	0.05	240	Commercial
A2	48.3	51.7	1.43	4.7	0.05	345	Modified
A3	48.3	51.7	1.43	4.7	0.1	346	Modified
A4	48.3	51.7	1.32	4.3	0.1	378	Modified
B1	46.7	56.3	1.67	3.8	0.06	245	Commercial
B2	46.3	53.7	1.63	4.3	0.05	287	Modified
B3	46.2	53.8	1.4	3.4	0.04	290	Modified
B4	46.2	53.8	1.66	3.8	0.1	240	Modified
C1	43.6	56.4	1.56	4.0	0.1	295	Commercial
C2	43.9	56.1	1.52	4.5	0.1	308	Modified
C3	43.9	56.1	1.41	4.5	0.09	345	Modified

increases with an increase of C_S or with addition of acids and with a decrease of C_V. For the constant C_V and temperature, the values of conductivity are defined mostly by the amount of free acid in electrolyte and can be roughly related to C_H.

2.2. Thermal Stability Screening Test of Electrolytes

To investigate thermal stability of electrolyte samples at higher (+40 to +65 °C) and lower (0 to −20 °C) temperatures, the electrolyte samples were prepared as series at high state-of-charge (SoC) (70–99%) and low SoC (0–20%) because positive and negative electrolytes at SoC values in these ranges are expected to be the most sensitive to temperature variations.[15]

A loss of vanadium electrolyte stability either because of recrystallization of vanadium salts or because of precipitation of vanadium pentoxide is a physicochemical process, which has its own kinetics.[7] Taking it into account, the thermal stability of electrolyte is defined in this study as an approximate time of exposure of electrolyte to a preset temperature without visible signs of aging such as precipitation or recrystallization. In other words, the stability is understood as an induction time of electrolyte aging. The results of visual inspection of positive and negative electrolyte samples are presented by mapping of their thermal stability in dependence on SoC value and temperature, as shown in **Figure 2**.

As shown in Figure 2a, the positive electrolytes obtained from commercial electrolyte samples A1 and B1, which have almost the same composition (Table 1), exhibit signs of instability at SoC higher than 80% and temperature higher than 55 °C or SoC higher than 90% starting from 50 °C. Positive and negative electrolytes from A1 and B1 remain stable at low temperatures. There were no visual changes or at least changes observed by naked eye for negative electrolyte samples at high temperatures. Electrolyte B2 has less vanadium ions and more sulfate species compared to the stock electrolyte B1, i.e., lower ratio C_V/C_S of 0.38 by comparison with 0.44 for B1 (As a stock electrolyte for each series A, B, or C was a commercial electrolyte and the total amount of free acid or protons remained unknown or cannot be estimated by instrumental analytical technique, the ratio C_V/C_H introduced by Liu et al.[7] could not be used for comparison or

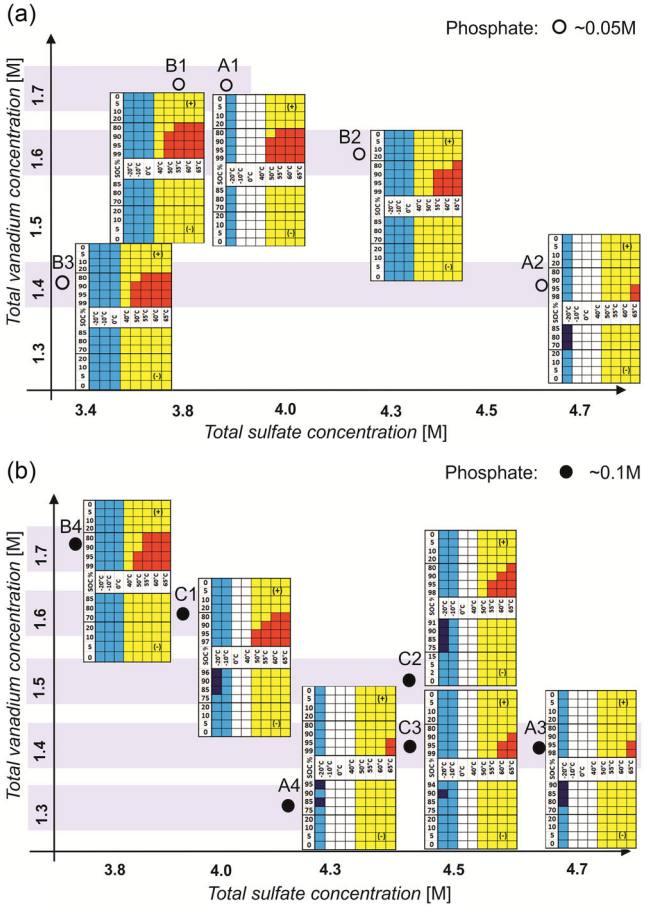

Figure 2. Graphic representation of thermal stability tests evaluation for series of electrolyte samples containing a) 0.05 M and b) 0.1 M of phosphate. Each diagram shows temperature and SoC values for positive (denoted as (+)) and negative (denoted as (–)) electrolyte samples. The color legend: yellow and light blue—there is no visual change after at least 3 days of electrolyte exposure to given temperature at given SoC, red—precipitation and dark blue—recrystallization occurred in less than 3 days, and white—no test has been performed.

interpretation of the results. Instead, we consider the ratio C_V/C_S, which can be derived from the analytical data for electrolyte series in Table 1.). The red-marked field, which corresponds to instability of B2 positive electrolyte, is smaller than that of B1. Thus, the reduction of C_V combined with an increase of C_S by addition of sulfuric acid results in stabilization of positive electrolyte and is consistent with the literature data.[19] Further, the stability of positive electrolyte A2, which has C_V/C_S ratio of 0.3, supports the tendency and only samples with SoC over 95% at 65 °C displayed signs of degradation within 3 days and are marked red in the chart (Figure 2a). However, the V(II) crystal formation occurred in A2 negative electrolyte samples of SoC from 70% to 85% at −20 °C. It can be explained by the effect of common ion, when high C_S affects the solubility of V(II) sulfate salts and promotes their recrystallization. It is interesting to note that dilution of electrolyte B1 by water to get electrolyte B3 does not change the C_V/C_S ratio and does not enhance the stability of positive B3 electrolyte at high temperatures compared to more concentrated B1 electrolyte.

Figure 2b shows the thermal stability chart for electrolyte series with 0.1 M total phosphate. It can be seen that positive electrolyte obtained from B4, which is characterized by the same C_V/C_S ratio as B1 but having more phosphate, is stabilized also at SoC of 90% at 50 °C in contrast to B1. The negative electrolyte from B4 as well as B1 displays no signs of optical or phase changes. Further decrease of C_V/C_s ratio to 0.39 (electrolyte C1) results both in a slight increase of positive electrolyte stability and in a limited stability or recrystallization in C1 negative electrolyte at −20 °C for SoC from 85% to 96%. The stability of electrolyte samples C2 (C_V/C_S is 0.34) matches the same tendency. Decrease of C_V to 1.4 M at the same C_S of 4.5 M narrows both the red- and dark blue-marked fields at the stability chart (Figure 2b) for electrolyte sample C3 compared to the sample C2. The smallest red-marked field at SoC of 95–98% and 65 °C for positive electrolyte can be seen in the case of A3 and the diagram looks like that one for A2. Electrolyte A4 is an example of the most diluted electrolyte in the series under consideration, where C_V/C_S ratio (0.31) is almost the same as for electrolyte A3 (0.3). Compared to the chart for A3, the ranges of thermal stability for A4 in terms of SoC and temperatures are very similar. In contrast to the signs of precipitation in positive electrolytes at high temperatures, which appear to correlate to C_V/C_S ratio, the appearance of solid phase in negative electrolytes at low temperatures does not seem to be systematically dependent on C_V/C_S ratio.

Recrystallization of V(II) solid species at −20 °C in A2, having 0.05 M of phosphoric acid, occurs at SoC of 70%. The negative electrolyte sample A3, containing 0.1 M of phosphoric acid at the same C_V/C_S ratio, displays the solid phase formation starting from SoC of 80%. Though the addition of phosphoric acid in the case of A3 seems to be stabilizing at low temperatures compared to A2, the precipitation of V(II) takes place also in the samples C1, C2, C3, and A4 from the series with 0.1 M of phosphoric acid at SoC of 75–85%. In contrast, the samples A1, B1, B2, and B3 at lower phosphoric acid concentration were stable at low temperatures. It is therefore difficult to derive any distinct effect of phosphoric concentration on the crystallization of V(II) at low temperatures from negative electrolytes of these series.

The stabilizing effect for positive electrolyte is likely to be a superposition of the stabilization due to phosphate additive and due to the sulfuric acid, i.e., due to the change of C_V/C_S ratio, especially at high C_V/C_S ratios. However, the effect of acid on thermal stability of positive electrolyte seems to be stronger than the effect of increasing phosphate concentration from 0.05 to 0.1 M.

To verify the results of visual inspection of negative electrolyte exposed to higher temperatures, an additional trial with subsequent titration of the electrolyte samples was carried out. Samples of A3 electrolyte for this trial were kept 3 weeks in a climate chamber at +60 °C and investigated to compare the concentration of vanadium species with the concentration in A3 samples stored at room temperature (**Table 2**).

As shown in Table 2, the C_V and molar content of V(V) and V(IV) species in positive electrolyte samples at SoC of 90% and 80% remained almost unchanged, indicating chemical stability of positive electrolyte after the trial. In contrast, the molar content of V(II) species in negative electrolyte samples at SoC of 86% and 77% (A3-80a, A3-70a in Table 2) decreased to 15%, whereas the molar content of V(III) increased to 15% whereby the C_V was constant.

This shift in V(III)/V(II) molar ratio at the constant C_V, i.e., conversion of V(II) in negative electrolyte, can generally be caused either by oxidation of V(II) by air or by reduction of protons or water by V(II) to evolve hydrogen. The oxidation of V(II) by oxygen from air is hardly possible unless the negative electrolyte is not kept under inert atmosphere. The reaction of V(II) with water is thermodynamically enabled under standard conditions, i.e., it does not require external driving force and is to distinguish from electrochemical hydrogen evolution side reaction, which occurs at the anode of VFB during battery operation. To ascertain the reason for V(II) oxidation in the samples of negative electrolytes during exposure to elevated temperature, the gas evolution from the electrolyte samples A3 was investigated by headspace online mass spectrometric (MS) technique.

2.3. Investigation of Chemical Stability of Negative Electrolyte by Direct Headspace Mass Spectroscopy

Two electrolyte formulations were chosen for the investigation of V(II) reactions in the negative electrolyte: A1 served as an example of a commercial electrolyte batch and A3 was taken as a formulation to get a stable positive electrolyte with enhanced thermal stability (Figure 2b). The samples of negative electrolyte A3 at SoC of 92% (A3-92a) and A1 at SoC of 96% (A1-96a) were brought into contact with a piece of carbon felt material in the

Table 2. Titration results for electrolyte samples after thermal stability trial. C_V is total vanadium concentration.

Sample	Reference values					Values after 3 weeks at +60 °C				
	Molar content [%]				C_V [M]	Molar content [%]				C_V [M]
	V(II)	V(III)	V(IV)	V(V)		V(II)	V(III)	V(IV)	V(V)	
A3-90c	–	–	≈10	≈90	1.45	–	–	11.2	88.8	1.45
A3-80c	–	–	≈20	≈80	1.45	–	–	20.4	79.6	1.49
A3-80a	85.7	14.3	–	–	1.41	70.9	29.1	–	–	1.41
A3-70a	76.7	23.3	–	–	1.41	62.0	38.0	–	–	1.42

sample vials in order to simulate the conditions of VFB, where electrolyte is continuously pumped through the felt electrodes.

Figure 3a shows the changes in ionic currents of analytes (gases) after the end of capillary of the mass spectrometer was placed into headspace gas phase above the negative electrolyte sample A3.

It can be seen that the measured signals of gases, which are components of air such as oxygen, argon, and carbon dioxide, decrease, whereas the signal of water vapor, nitrogen, and hydrogen increases. Nitrogen gas was initially in the headspace of the sample and its signal rises up and decreases slowly. The decrease of the nitrogen signal is caused by vacuum, which is created slowly in the course of the evacuation of the gas phase during the measurement step. The signal of hydrogen rises first strongly and then falls slowly down in contrast to the signal of water, which rises slowly and continuously. It indicates that a small amount of hydrogen was accumulated in the glass vial with electrolyte at room temperature and can be formed by the reaction of V(II) with protons. The amount of hydrogen gas evolved in the headspace during the gas detection step was 200 ppm and was estimated related to the nitrogen gas. This gas amount cannot be taken as an absolute value for gas concentration, but it allows the comparison of vanadium electrolyte formulations. After the negative electrolyte A3 was kept during 1 h at 50 °C, the amount of hydrogen gas detected in the headspace increased to 500 ppm (Figure 3b). More prolonged heating of the A3 sample at 50 °C, i.e., over 18 h, leads to the detection of 3000 ppm of hydrogen gas in the headspace of glass vial (Figure 3c).

Electrolyte sample A1 contains more vanadium, less sulfate, and therefore less free acid. The run of the curves shown in **Figure 4**a for the sample A1 at room temperature is similar to that shown in Figure 3a for A3. However, the amount of hydrogen evolved from A1 at room temperature is 100 ppm, which is less than that in case of A3 electrolyte. After the first measurement, the vacuum has been produced in the sample vial and the signal for nitrogen in the course of the following measurements decreased (Figure 4b,c).

The generation of vacuum was taken into account for quantitative evaluation of hydrogen gas amount. The heating of the

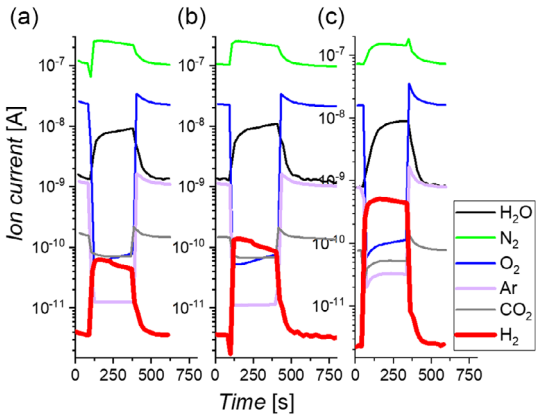

Figure 3. The online MS analysis of gas samples from the headspace over A3-92a electrolyte after the glass vial with electrolyte was kept a) at room temperature, b) at +50 °C for 1 h, and c) at +50 °C for 19 h. Amount of detected hydrogen in ppm is a) 200, b) 500, and c) 3000.

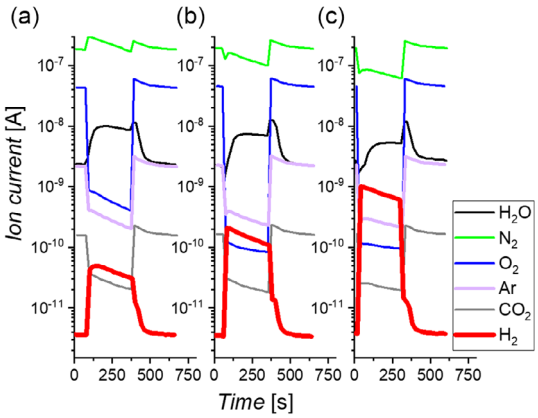

Figure 4. The online MS analysis of gas samples from the headspace over A1-96a electrolyte after the glass vial with electrolyte was kept a) at room temperature, b) at +50 °C for one hour, and c) at +50 °C for 19 h. Amount of detected hydrogen in ppm is a) 100, b) 1100, and c) 10 000.

sample A1 during 1 or 18 h produced several times more hydrogen gas (1100 and 10 000 ppm) compared to the sample A3 under the same conditions. Thus, the instability of negative electrolyte because of chemically generated hydrogen evolution reaction seems to be also dependent on C_V/C_S ratio. A more systematical study is needed to reveal this dependence. It can be expected that besides electrochemical side reaction leading to hydrogen gas evolution, generation of hydrogen gas can proceed chemically at elevated temperatures at considerable rate even if this reaction can be neglected at room temperature. The electrolyte development strategy of C_V/C_S ratio optimization to improve thermal stability of vanadium positive electrolyte should be accompanied by the investigation of gas evolution from negative electrolyte.

2.4. Charge–Discharge Cell Test

The charge–discharge cell test was designed in such a way that a relative small amount of electrolyte (60 mL in each tank) was used for a cell with geometric surface of 40 cm^2. This design is advantageous to compare the electrolytes under more severe conditions and to realize their tendency to performance loss or limitations. The cells with electrolytes A1 and A3 were charged and discharged at the current densities from 25 to 70 mA cm^{-1}. The Coulombic efficiency (CE) derived from charge–discharge curves (**Figure 5**) was about 98–99% for both of the cells.

The cell operated with electrolyte A3 is characterized by higher EE in the whole range of current densities under consideration. As both of the cells displayed the same CE, the difference in EE is due to the difference in voltage efficiency. Assuming that the kinetic and transport losses could be the same for both cells, the difference in voltage efficiency can result from difference in internal cell resistance and therefore from ohmic losses. The vanadium electrolyte is known to contribute to a large extent to the internal cell resistance. Provided that the electrode and membrane materials were the same, the difference in voltage efficiency can be caused by difference in electrolytes conductivity (Table 1). In fact, the internal cell resistance measured before charge–discharge test was 72 mΩ for cell A1 and 59 mΩ for cell

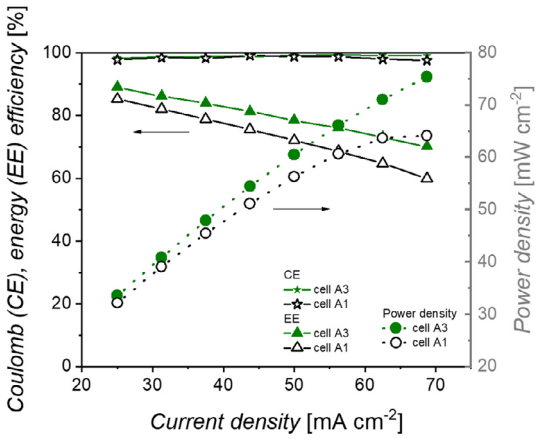

Figure 5. Discharge power density, EE, and CE in dependence on current density for the cells operated with (cell A1) electrolyte A1 and (cell A3) electrolyte A3.

A3. The discharge power density curve for the cell A1 shown in Figure 5 displays no further increase of values at current densities higher than 63 mA cm^{-1}. Compared to the cell A1, the cell operated with electrolyte A3 exhibits continuous increase of power density with an increase of current density of galvanostatic discharge step.

The cell capacities are shown in dependence on cycles number, as shown in **Figure 6**.

As it was expected, the initial discharge capacity of the cell A1 is higher than that of the cell A3 due to the higher total vanadium concentration of electrolyte A1 compared to the electrolyte A3 (Table 1). After consequent charge–discharge cycles with an increase of current density, the discharge capacity of both cells was almost equal and finally the cell A3 retained more discharge capacity than the cell A1. Thus, the cell with electrolyte A1 exhibited stronger discharge capacity decay.

It remains unclear if more stable operation of the cell A3 compared to the cell A1 can be attributed to higher electrolyte conductivity or to the effect of C_V/C_S ratio on the transport

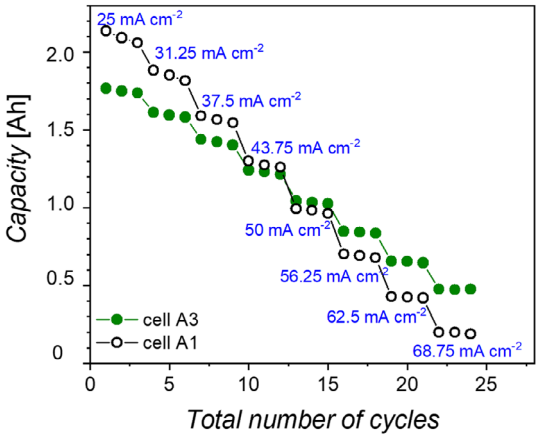

Figure 6. Discharge capacity of the cells operated with (cell A1) electrolyte A1 and (cell A3) electrolyte A3 during galvanostatic charge–discharge cycles at various current densities (shown in blue).

processes, or electrochemical reactions in the VFB or to both of them. In addition, based on the investigation of thermal stability of vanadium electrolytes, the electrolyte formulation A3 seems to be more preferable than A1 for the long-term VFB operation in a broad temperature range in terms of stability and cyclability.

3. Conclusion

The series of positive and negative electrolytes at various SoC have been prepared by electrolysis of electrolyte samples at C_V in the range from 1.4 to 1.7 M and C_S from 3.8 to 4.7 M. The concentration of phosphate as additive was maintained in the range from 1.4 to 1.7 M throughout these series. The ex situ stability of electrolyte at low temperatures (−20 °C) is limited by recrystallization of vanadium(II) salts in negative electrolyte, which is consistent with the literature data. At high temperatures (+50–65 °C), the electrolyte aging or decomposition is found to be caused not only by precipitation of vanadium pentoxide in positive electrolyte, but also by slow hydrogen gas evolution in negative electrolyte at least at SoC above 80%. The hydrogen gas evolution can be attributed to homogeneous reaction of vanadium(II) with protons and can result in about 15% loss of SoC after 3 weeks of heating of electrolyte at +60 °C. The thermal stability of positive electrolyte at elevated temperature is assumed to correlate with C_V/C_S ratio and conductivity, so that an electrolyte evaluation based on the measurement of C_V, C_S, and conductivity can be used to predict the electrolyte aging at high SoC and various operation temperatures. The effect of C_V/C_S ratio to thermal stability of positive electrolyte is likely to be superior to the effect of phosphate stabilizing agent at least at C_P in the range from 0.05 to 0.1 M.

The application of diluted vanadium electrolyte (C_V of 1.4 M and C_P of 0.1 M) can be reasonable to improve battery cyclability during galvanostatic charge–discharge operation in terms of capacity decay and ohmic losses. For double-function applications of VFB, where vanadium electrolyte is used also as a heat exchanger or for operation of VFB at elevated temperatures, it is necessary to monitor hydrogen gas evolution in negative half-cell and adjust electrolyte formulation.

4. Experimental Section

Chemicals: Sulfuric acid (95%, supra) was Carl-Roth reagent; phosphoric acid (85%, Ph. Eur. p.a.) was a VWR reagent. Batches of commercial vanadium electrolyte (in $V^{3.5+}$ oxidation state [commercial vanadium electrolyte contains V(III) and V(IV) species in molar ratio close to 50:50% and is therefore denoted as $V^{3.5+}$ electrolyte]) were purchased from AMG TITANIUM ALLOWS & COATINGS GfE Metalle und Materialien GmbH.

Electrolyte Preparation: Three batches of commercial $V^{3.5+}$ electrolytes were used as a stock to prepare modified electrolytes (batches A1, B1, and C1 in Table 1). The analysis of A1, B1, and C1 electrolytes composition for impurities is given in Table S2, Supporting Information. As no standard specification is currently available for vanadium electrolyte solution, the batches with C_V in the range from 1.5 and 1.7 M were chosen for this study. The batches were further analyzed to determine total sulfate concentration and conductivity. The total phosphate concentration was taken from the data, provided by supplier. Modified $V^{3.5+}$ electrolyte samples were obtained by dilution of stock electrolyte batches by water with addition of calculated amounts of concentrated sulfuric and phosphoric acids to

achieve final C_V, C_S, and phosphate concentrations. A total of 11 $V^{3.5+}$ vanadium electrolyte samples were investigated in this study, including three commercial electrolyte batches (Table 1). $V^{3.5+}$ electrolytes were converted into V(III), V(II), V(IV), and V(V) redox forms of electrolyte by electrolysis. The electrolysis was carried out in a 40 cm^2 cell of the same design as described in part 4.4 for the cell test. A galvanostatic–potentiostatic mode with maximal voltage of 1.65 V and maximal current of 3 A was applied to charge the cell with electrolyte sample, whereby the end-of-charge voltage was set to 1.65 V for galvanostatic step at 75 mA cm^{-2} and then the cutoff current was 10 mA cm^{-2} at applied voltage of 1.65 V.

Samples of negative and positive electrolyte at various SoC values were prepared by mixing of the calculated volumes of V(II) and V(III) samples and V(IV) and V(V) samples, correspondingly. The expected values of SoC and C_V for these electrolyte samples are given in Table S1, Supporting Information. A check of SoC for selected electrolyte probes by titration shows that there can be deviation of about 3% for the calculated values from experimental ones. This deviation in SOC values is considered to be negligible to find the correlation between electrolyte thermal stability and SOC.

Determination of Total Vanadium and Sulfate Concentrations: Total vanadium concentration and molar ratio of vanadium species in various oxidation states were determined by potentiometric titration using 0.1 M cerium(IV) sulfate standard solution (Carl-Roth, Germany). The titration was carried out by means of automatic titrator T70 (Mettler Toledo Int. Inc., Germany). Classical gravimetric procedure based on precipitation with barium chloride was used to determine total concentration of sulfate.

Conductivity Measurement: Electrolyte conductivity was measured using AC impedance technique in a four-electrode glass cell with a cell of 7.3 cm^{-1} and glassy carbon or graphite electrodes. The measurement of high-frequency resistance values was carried out in a frequency range from 10 to 100 kHz with AC of 10 mA and 0 DC. A standard solution with conductivity of 500 mS cm^{-1} was used for calibration of the cell.

Ex Situ Thermal Stability Test: To estimate thermal stability of positive and negative electrolyte, the electrolyte samples of 1 mL in closed plastic vials were exposed to a preset temperature in a test chamber (Weiss WKL 64, Germany) for a certain period of time. Unless otherwise noted, the trials were conducted in a such way that the temperature has been set up stepwise from room temperature to +65 °C or from room temperature to −20 °C and was held for 3 days at each step. The samples were visually inspected during the test trial for the signs of degradations such as precipitation, sediment formation, and color change. The composition of selected electrolyte samples after the thermal stability trial was analyzed by titration.

Charge–Discharge Experiments: Galvanostatic charge–discharge test was carried out in a cell with 40 cm^2 geometric surface at room temperature using a Gamry Reference 3000 potentiostat. The following materials were used to assemble the cell: Fumasep FAP-450 membrane (FuMa-Tech GmbH, Germany) as separator, surface-treated GFD 4.6 graphite felt SIGRACELL (SGL Group, Germany), and FU 4369 graphite bipolar plates (Schunk Kohlenstofftechnik GmbH, Germany) as electrode and current collector. Felt electrodes and membrane were disposable materials and were replaced by new ones for each cell. The electrolyte flow rate was 75–80 mL min^{-1} and 60 mL of $V^{3.5+}$ electrolyte was used in each tank. The cell was kept at open-circuit voltage for 2 min between the charge–discharge cycles. Three charge–discharge cycles with cutoff voltages of 1.65 and 0.8 V, respectively, were performed for each current density in the range from 25 to 70 mA cm^{-1}.

Internal cell resistance was determined by galvanostatic electrochemical impedance spectroscopy technique (EIS). The EIS measurement was performed before any charge–discharge experiment at zero direct current and 10 mA amplitude of alternating current in the frequency range from 0.1 to 10^5 Hz.

Direct Headspace MS (Online MS) Investigation: Analysis of the gas products formed in the glass vials containing negative electrolyte samples was carried out using a quadrupole QMG 700 mass spectrometer with conventional electron impact ionization (Pfeiffer Vacuum GmbH, Germany). The ion source was a tungsten cathode.

Two pieces of felt material with the total weight of 0.14 g used as electrode for VFB assembly were brought into contact with 7 mL of electrolyte sample in the glass vial of 40 mL volume in an air-free environment, i.e., in a glove box filled with nitrogen gas. The glass vials were sealed with a teflon-coated silicon septum cap and taken out from the glove box. The pieces of felt in electrolyte were used in this experiment to simulate real conditions in VFB, where the negative electrolyte is fed or pumped through the felt electrode during battery operation. If it was necessary, the vials with electrolyte samples were placed in a thermostat and were cooled down to the room temperature before the headspace gas was sucked of the vial through the sniffing capillary of the online mass spectrometer and was analyzed online. This step was of 5 min duration. The capillary had a stainless needle to pierce through the teflon-coated septum. The headspace of the vials was not ventilated, so that there was a vacuum about 500 mbar after the headspace gas was taken into capillary. Between the headspace measurements of the different samples, the capillary was flushed with atmospheric air, i.e., atmospheric air was injected into mass spectrometer through the withdrawn sniffer capillary.

Selected masses representing the gas components of the gas mixture were measured versus time. The dwell time for each mass was 1 s. The t-90 response time was 0.3 s. The hydrogen gas concentration was calculated related to the concentration of nitrogen gas in the headspace of the sample vial, taking into account vacuum formation.

Supporting Information

Supporting Information is available from the Wiley Online Library or from the author.

Acknowledgements

This work was financially supported by the German Federal Ministry for Economic Affairs and Energy (BMWi) in the context of the project "BiFlow" (03EI3025B). The responsibility for the content of this publication lies with the authors. The authors are grateful to Dr. Frank Säuberlich, Dr. Meiser Valencia (1st Flow Energy Solutions GmbH, Germany), and Nina Munzke, Dr-Ing. Christian Kupper (Karlsruhe Institute of Technology, Germany) for fruitful discussions in this work.

Open Access funding enabled and organized by Projekt DEAL.

Conflict of Interest

The authors declare no conflict of interest.

Data Availability Statement

The data that support the findings of this study are available from the corresponding author upon reasonable request.

Keywords

electrolytes, side reactions, thermal stability, vanadium flow batteries

Received: July 3, 2023
Revised: September 8, 2023
Published online: October 16, 2023

[1] J. Marschewski, L. Brenner, N. Ebejer, P. Ruch, B. Michel, D. Poulikakos, *Energy Environ. Sci.* **2017**, *10*, 780.

[2] a) A. Bhattarai, N. Wai, R. Schweiss, A. Whitehead, G. G. Scherer, P. C. Ghimire, T. M. Lim, H. H. Hng, *Appl. Energy* **2019**, *236*, 437;

b) A. Trovò, A. Saccardo, M. Giomo, M. Guarnieri, *J. Power Sources* **2019**, *424*, 204.
[3] A. Bhattacharjee, A. Roy, N. Banerjee, S. Patra, H. Saha, *J. Power Sources* **2018**, *396*, 506.
[4] C. Choi, S. Kim, R. Kim, Y. Choi, S. Kim, H.-Y. Jung, J. H. Yang, H.-T. Kim, *Renewable Sustainable Energy Rev.* **2017**, *69*, 263.
[5] D. N. Buckley, D. Oboroceanu, N. Quill, C. Lenihan, R. P. Lynch, *J. Electrochem. Soc.* **2021**, *168*, 30530.
[6] D. K. Kim, S. J. Yoon, S. Kim, *Int. J. Heat Mass Transfer* **2020**, *148*, 119040.
[7] Y. Liu, L. Yu, L. Liu, J. Xi, *Appl. Energy* **2021**, *301*, 117454.
[8] N. Roznyatovskaya, K. Pinkwart, J. Tübke, in *Flow Batteries- From Fundamentals to Applications*, Vol. *1* (Eds: C. Roth, J. Noack, M. Skyllas-Kazacos), Wiley-VCH, Weinheim, Germany **2022**, Ch. 4.
[9] Y. Song, X. Li, C. Yan, A. Tang, *J. Power Sources* **2020**, *480*, 229141.
[10] M. Jing, Z. Wei, W. Su, H. He, X. Fan, Y. Qin, J. Liu, C. Yan, *J. Power Sources* **2016**, *324*, 215.
[11] A. Fetyan, G. A. El-Nagar, I. Lauermann, M. Schnucklake, J. Schneider, C. Roth, *J. Energy Chem.* **2018**, *32*, 57.
[12] C.-N. Sun, F. M. Delnick, L. Baggetto, G. M. Veith, T. A. Zawodzinski, *J. Power Sources* **2014**, *248*, 560.
[13] J. Lee, J. T. Muya, H. Chung, J. Chang, *ACS Appl. Mater. Interfaces* **2019**, *11*, 42066.
[14] T. Greese, G. Reichenauer, *J. Power Sources* **2021**, *500*, 229958.
[15] K. Wang, Y. Zhang, L. Liu, J. Xi, Z. Wu, X. Qiu, *Electrochim. Acta* **2018**, *259*, 11.
[16] Y. Wen, Y. Xu, J. Cheng, G. Cao, Y. Yang, *Electrochim. Acta* **2013**, *96*, 268.
[17] Y. Zhao, L. Liu, X. Qiu, J. Xi, *Electrochim. Acta* **2019**, *303*, 21.
[18] N. V. Roznyatovskaya, V. A. Roznyatovsky, C.-C. Höhne, M. Fühl, T. Gerber, M. Küttinger, J. Noack, P. Fischer, K. Pinkwart, J. Tübke, *J. Power Sources* **2017**, *363*, 234.
[19] E. H. Kirk, F. Fenini, S. N. Oreiro, A. Bentien, *Batteries* **2021**, *7*, 87.